THE JOURNAL OF PHYSICAL CHEMISTRY Letters

Perspective

pubs.acs.org/JPCL

Emerging Physicochemical Phenomena along with New Opportunities at the Biomolecular−Nanoparticle Interface

Allison M. Dennis,[†] James B. Delehanty,[‡] and Igor L. Medintz*[,‡]

[†]Department of Biomedical Engineering, Boston University, 44 Cummington Mall, Boston, Massachusetts 02215, United States

[‡]Center for Bio/Molecular Science and Engineering, Code 6900, U.S. Naval Research Laboratory, 4555 Overlook Avenue, Southwest, Washington, District of Columbia 20375, United States

ABSTRACT: Efforts to create new nanoparticle−biomolecule hybrids for diverse applications including biosensing, theranostics, drug delivery, and even biocomputation continue to grow at an unprecedented rate. As the composite designs become more sophisticated, new and unanticipated physicochemical phenomena are emerging at the nanomaterial−biological interface. These phenomena arise from two interrelated factors, namely, the novel architecture of nanoparticle bioconjugates and the unique physicochemical properties of their interfacial environment. Here we examine how the augmented functionality imparted by such hybrid structures, including accessing concentric energy transfer, enhanced enzymatic activity, and sensitivity to electric fields, is leading to new applications. We discuss some lesser-understood phenomena that arise at the nanoparticle interface, such as the complex and confounding issue of protein corona formation, along with their unexpected benefits. Overall, understanding these complex phenomena will improve the design of composite materials while uncovering new opportunities for their application.

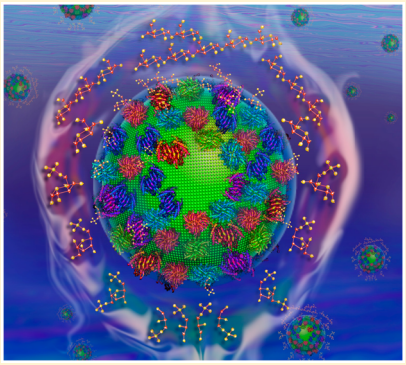

Integrating inorganic nanoparticles (NPs) and biomolecules into hybrid materials exhibiting a growing range of functional complexities has been a primary and recurring theme in nanobiotechnology since before that term existed. In an example of a very early hybrid, the adsorption of protein onto the negatively charged surface of gold nanoparticles (AuNPs) was used to stabilize the resulting bioconjugates in diverse electrolyte solutions by changing the mechanism of colloidal stability from electrostatic repulsion to steric hindrance.[1] In 1971, the nonspecific adsorption of antibodies onto the surface of colloidal gold yielded a new composite material with added functionality, leading to the ongoing use of antibody-labeled AuNPs as an immunostain for transmission electron microscopy (TEM).[2] Although this example makes clear that the concept of integrating NPs and biomolecules is hardly new, the contemporary literature contains numerous examples of increasingly complex functional hybrid devices that take advantage of an expanding range of NP compositions and surface chemistries as well as evolving NP−biomolecule assembly approaches.[3−7] While a comprehensive discussion of this expansive field is beyond the scope of this Perspective, it is important to note the diversity of the nanocomposites, their range of potential applications, and the amount of research being invested in them.[8] In many cases, these applications would appear to the uninformed reader to be the stuff of science fiction. The creation of a targeted nanomedicine meant to overcome issues associated with systemic drug delivery is a primary example. Here a NP vector would utilize an antibody for targeting and some type of controlled release mechanism to provide therapy at a specific site while also providing contrast for multimodal imaging and perhaps even biosensing of the localized environment over time.[9] Alternatively, we can envision stand-alone NP-based sensing devices capable of rudimentary information processing to provide useful information beyond just the equivalent of raw telemetry (by stand-off optical or electronic interrogation).[10,11] In this Perspective, we discuss two interrelated subjects directly linked to the nanomaterial−biomolecular interface. First, we address the previously unanticipated phenomena and opportunities arising at this interface—in many cases as a direct result of the unique hybrid architecture—that are leading to new biocomposite nanomaterials and applications. Second, we discuss how the NP−biomolecule interface manifests a unique and largely uncharacterized local environment that directly impacts the presentation of surface ligands, ion concentrations, diffusion, and resulting biomolecular activity when compared to either a flat surface (i.e., film or bulk solid) or a solution. Following introduction of some important supporting concepts, the first point is illustrated in the context of some descriptive examples from the recent literature. This is followed by an overview of the second topic along with an example involving attaching enzymes to NPs that appears to benefit directly from it.

Nanoparticulate bioconjugates are, in essence, any combination of NP and biomolecule(s). Typical inorganic or hard NPs include those derived from metals (e.g., gold, silver), semiconductors (e.g., quantum dots (QDs)), carbon dots, carbon nanotubes, or oxides (e.g., iron oxide), while organic or soft

Received: March 11, 2016
Accepted: May 17, 2016
Published: May 24, 2016

DOI: 10.1021/acs.jpclett.6b00570
J. Phys. Chem. Lett. 2016, 7, 2139−2150

NPs include polymers, liposomes, micelles, cellulosic NPs, and even those originating from DNA.[5,12−14] Depending on the composition and size of these NPs (ca. 1−100 nm in diameter), unique properties emerge due to quantum confinement, including, for example, the size-tunable photoluminescence (PL) of QDs, the ballistic conductivity of carbon allotropes such as single-wall carbon nanotubes and graphene, the magnetic resonance of metal oxides, and the Raman enhancement, surface plasmon resonance (SPR), and photothermal effects of AuNPs.[5−7] The physical structure of NPs is distinct from that of either molecules or bulk materials, resulting in unique interactions with the surrounding environment. These interactions cannot be described using models designed for a bulk surface or freely diffusing molecule but rather require something in-between with unique characteristics of its own.[15−18] The NP can be used as a substrate to anchor a biomolecule, similar to a bulk surface, but will still diffuse through solutions like a soluble molecule, although typically at a much slower rate. As a central nanoscaffold, the NP provides a nontrivial surface area with multiple binding sites for biomolecular tethering, which can provide access to multivalency and high local avidity, while the nanoscale radius of curvature presents a morphology distinct from bulk materials, films, or even microspheres.[15−17] Figure 1 presents a schematic

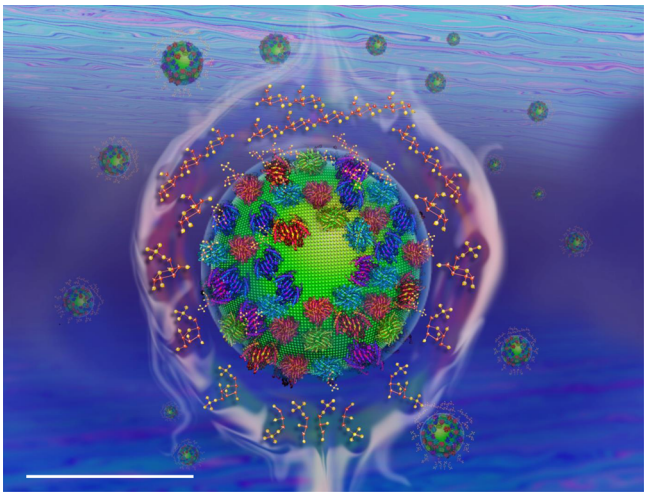

Figure 1. Schematic representation of the nanobioconjugate localized environment. The image shows a semiconductor quantum dot (QD) in green (~6 nm diameter, size bar) displaying multiple copies of different enzymes involved in glycolysis for potential utility in ethanol fermentation. A unique, high-avidity, nanoscale architecture is enabled by the high local concentration of enzymes. The unique localized environment around these hybrid composite materials, which is starkly different from the bulk solution, is schematically highlighted by the pink halo placed around the construct. The light blue semitransparent sphere around the QD−enzyme conjugate represents the surface ligands utilized to make the QDs colloidally stable. These ligands also have a profound influence on the local conjugate environment.

of a QD assembled with multiple copies of several different glycolytic enzymes (to scale) to highlight both the unique architecture and potential for high-avidity presentation. The desire to combine biological properties and this unique NP morphology, not to mention the extra functionality imparted by the properties of the NP (e.g., paramagnetism or fluorescence) as noted above, is driving the accelerating interest in a myriad of applications utilizing bionanocomposites. It is important to note that many intrinsic features of the NP bioconjugate will be directly relevant to and influence the function of this and similarly utilized NP scaffolds, including the localized NP environment, NP composition, NP size and shape, coating and surface chemistry, ligand density, protein adsorption, interaction with solvent, nature of the biomolecule, biomolecular orientation, surface charge, and so forth; further discussion of these issues can be found in refs 15−17.

The physical structure of NPs is distinct from that of either molecules or bulk materials, resulting in unique interactions with the surrounding environment.

As synthesized, many NPs are not colloidally stable in water and require surface modifications to be stably dispersed in biological media. Chemically modifying or replacing the native NP surface to display ligands that mediate solubility through charge or steric hindrance/repulsion enables water miscibility. The hybrid structure is formed when the biological (e.g., protein, peptide, nucleic acid, drug, etc.) is attached to the NP surface. This necessitates bioconjugation chemistries, which can encompass electrostatic or hydrophobic/hydrophilic interactions, chelation, dative coordination, covalent modification, or even incorporation during synthesis. Ideal nanobioconjugation chemistry enables biomolecule−NP coupling with control over the affinity, stoichiometry, orientation, and proximity of the biomoieties with high reproducibility while remaining generalizable across both a wide variety of nanomaterials and biologicals.[15,18−20] In practice, precise, high-yield bioconjugation produces more effective nanobiocomposites with less material. For in-depth analysis of these complex issues, the interested reader is referred to some relevant literature.[15,18−20] Different coating types also strongly influence the nature of how biomolecules, especially proteins, nonspecifically interact with the NPs. Relevant issues here are the type of coating molecules and their sizes, amphiphilicity, charge, hydrophobicity, and other physiochemical properties (e.g., stiffness, compaction, etc.). These effects and the issues subsequently encountered with them can be drastically amplified when accessing the intracellular environment.[21,22]

In many examples, bioconjugation of NPs leads to the creation of high-avidity constructs with multiple biomolecules densely displayed around a nanoscale, high surface-to-volume (S/V) scaffold.[15,18−20] This particular architecture has already been extensively exploited to some extent in the context of enzyme applications, antibody assays, and many other NP bioconjugates.[23] For example, enzyme-conjugated magnetic NPs allow for the application and then removal of an immobilized protein catalyst for further substrate processing and subsequent catalytic reuse.[24] Similarly, antibody-conjugated magnetic NPs facilitate the capture and enrichment of low-abundance antigens or, alternatively, improvements in the sensitivity and limits of detection (LOD) of enzyme-linked immunosorbent assays (ELISAs).[25]

The multivalency of a NP bioconjugate has a direct impact on the functionality of any hybrid device as it acts to aggregate biomolecules on the particle surface. This serves as either an advantage or a detriment, depending on the application at hand. For example, highly scattering AuNPs or fluorescent QDs

DOI: 10.1021/acs.jpclett.6b00570
J. Phys. Chem. Lett. 2016, 7, 2139−2150

have been used for single-particle tracking studies in cellular imaging, yielding new insights into receptor−ligand binding and molecular trafficking in cells.[26,27] It has been observed, however, that the binding of a NP to a particular receptor slows its natural diffusion rate due to both the drag of the particle (which is related to its overall size) and when the particle displays multiple tethering points (e.g., displaying multiple ligands for a cell surface receptor). When the NP binds multiple moieties, it effectively cross-links them, perturbing the molecular dynamics under observation.[28] Advanced bioconjugation strategies have been developed to specifically label NPs with exactly one biomolecule, generating monovalent nanobioconjugates for these specific applications.[29]

The Mirkin Group's seminal work utilizing DNA-functionalized AuNPs for colorimetric detection of DNA sequences by alteration of the NP's SPR highlights how a unique NP bioconjugate architecture can lead to new applications.[30] It also underlines the yin and yang or dual benefit/liability nature of this area as, paradoxically, dense functionalization of AuNPs with DNA can be both beneficial or deleterious, depending on the context. For example, dense DNA functionalization on a NP protects the conjugate from nuclease activity by sterically blocking enzyme binding but can simultaneously preclude efficient hybridization.[31] Protection from nuclease activity has, in turn, given rise to research focused on the therapeutic delivery of nucleic acids in analogous high-avidity conformations that seek to exploit other unique properties provided by these composite materials.[32] For example, sophisticated gene transfection vehicles aimed at combining DNA-condensing capability, the buffering capacity of polymers like polyethylenimine (PEI), and magnetic or paramagnetic NPs (MNPs) are being developed as nonviral gene transfection agents that can be magnetically directed to specific tissues. It has been shown that gene transfection efficiency is higher with PEI−plasmid DNA (pDNA) complexes bound to paramagnetic iron oxide MNPs even in the absence of a magnetic field.[33] When anchored to the MNP, PEI−pDNA dissociates more slowly, but more completely, releasing far more pDNA into the cell. PEI bound to the MNP is excluded from the cell nucleus, while the pDNA released from the complex localizes in and around the nucleus; this spatial separation of PEI and pDNA improved transfection efficiency and reduced toxicity compared to PEI−pDNA without the NP scaffold. This example highlights the specific impact of how the choice of a chemically functionalized nanoscaffold can uniquely contribute to device function.

Nanoscaffold multivalency can also directly impact the success of a hybrid nanobio device, as with Förster resonance energy transfer (FRET)-based devices utilizing fluorescent QDs. QDs are popular FRET donors because of their tunable PL, brightness, high quantum yield, and broad absorption spectra, which can be cumulatively used to minimize direct acceptor excitation.[34,35] However, in direct contrast to most conventional single-donor−single-acceptor FRET assemblies, the nontrivial QD size and high S/V ratio allow multiple discrete acceptor moieties to be displayed around the nanocrystal.[34] This unique configuration allows the resultant intra-assembly FRET efficiency to be controlled and even "dialed in" as it proportionally increases the effective FRET acceptor absorption cross section. This assumes a centrosymmetric placement of the acceptor around the QD donor; heterogeneous acceptor placement makes this situation far more complex because the acceptors closest to the QD will dominate FRET interactions. Within these multivalent systems, the equation relating FRET efficiency (E) to the donor−acceptor distance (r) and the Förster distance (R_0, the characteristic distance for a given donor−acceptor pair at which the energy transfer (ET) efficiency is 50%) is modified to adjust for the number of acceptors per donor (n) as follows[34]

$$E(n) = \frac{nR_0^6}{nR_0^6 + r^6} \tag{1}$$

The effect of this configuration on FRET E is schematically highlighted in Figure 2.[36] In practice, controllably increasing

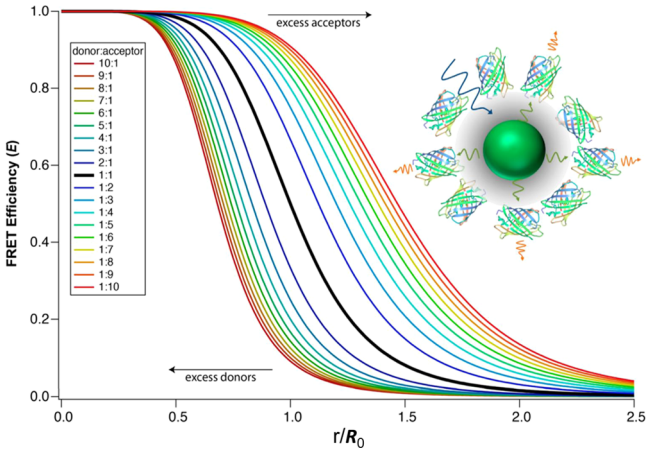

Figure 2. Representative simulation meant to impart the distance dependence of FRET efficiency for multivalent systems based loosely on eq 1. The FRET efficiency at a given distance improves as the number of acceptors per donor, n, increases and vice versa. The inset shows an example of such a multivalent system; multiple fluorescent protein acceptors are bound to a single QD donor. Reproduced from ref 36 with permission of MDPI under the Creative Commons Attribution License.

the number of acceptors per donor increases the effective or apparent R_0 of the multivalent system, and this manifests as an increase in the potential length scale over which one can induce a measurable change in the fluorescent signal.[34] These effective/apparent "increases" in acceptor cross section and R_0 occur if one treats the multiple, indistinguishable acceptor molecules as behaving as one aggregate acceptor, a concept that is not easily transferred mathematically. In contrast, increasing the number of discrete donors per QD only increases the probability of FRET (i.e., the probability of energy arriving at an acceptor as opposed to leaving the donor) as the QD acceptor can only couple with a single donor dipole per transfer event.[34,37] The bioconjugation strategies employed to generate these devices (and the stoichiometry and orientation of the final product) are critical to their function. Molecular systems can be precisely labeled with multiple acceptors per donor by saturating a fixed number of potential binding sites, but a nanoscaffold typically exhibits a less determinate number of binding sites and is rarely saturated; therefore, one must account for a range of labeling stoichiometries. Single-particle FRET studies have demonstrated that the number of acceptors per QD donor closely follows a classical Poisson distribution, and any heterogeneity in the resulting ensemble can be accounted for mathematically. The latter is usually only necessary at low acceptor per QD ratios as at larger ratios ($\geq$4), the distribution usually starts to match more closely with Poissonian expectations.[37]

DOI: 10.1021/acs.jpclett.6b00570
J. Phys. Chem. Lett. 2016, 7, 2139−2150

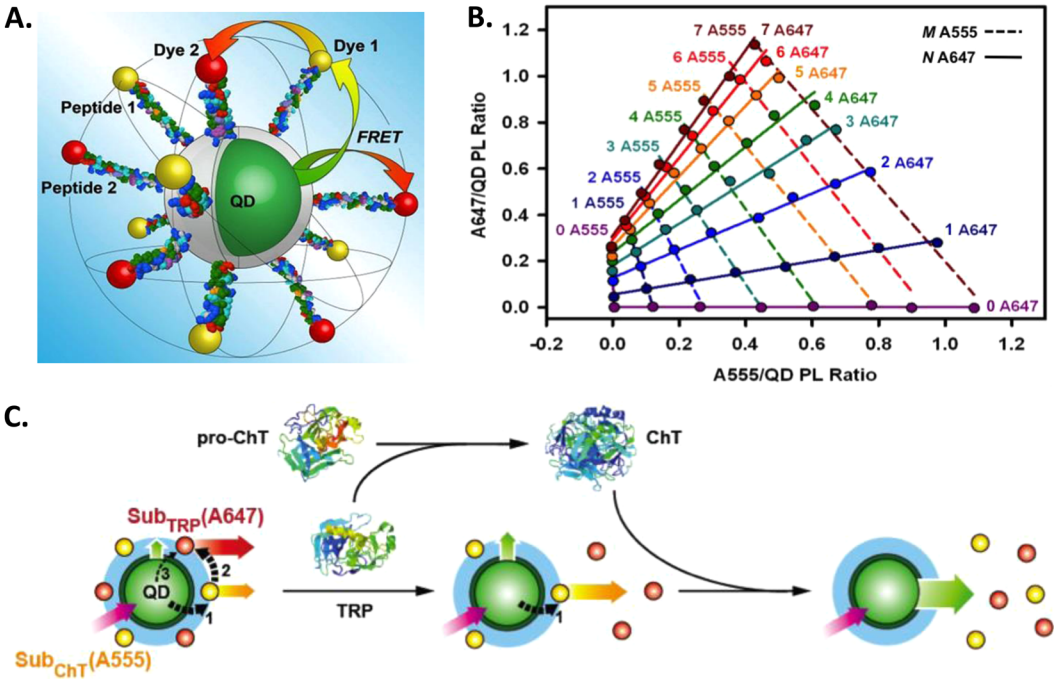

Figure 3. (A) Central QD engaged in cFRET with multiple dye acceptors arranged symmetrically around its surface. In this example, the dyes are attached to peptides displayed on the QD. Multiple ET routes exist, including QD-to-dye and dye-to-dye pathways. Reproduced from ref 76 under the Creative Commons Attribution-Noncommercial 3.0 Unported License. (B) A647/QD PL ratios plotted versus A555/QD PL ratios. Each combination of PL ratios (i.e., point on the plot) corresponds to a unique combination (*M*,*N*). (C) Schematic of the pro-ChT activation sensing experiment that monitors TRP activity and Pro-ChT conversion to active ChT with $FRET_1$, $FRET_2$, and $FRET_3$ indicated by 1, 2, and 3, respectively. Panels B and C reproduced from ref 38, copyright 2012 American Chemical Society.

The concept of QD-based concentric FRET (cFRET) arises directly out of this single QD donor/multiple acceptor configuration and can be considered another prototypical example of how the unique NP architecture leads to new applications. In a cFRET configuration, multiple copies of two or more different FRET acceptors surround the central donor QD, establishing multiple sequential or competitive ET pathways (Figure 3A). When implemented with functional biomolecular linkages or bridges (e.g., complementary DNA sequences or protease cleavage sequences) and a judicious combination of acceptor dyes, the multiple FRET pathways present in cFRET configurations provide the basis for new types of biosensors.

The simplest cFRET configuration implemented to date consists of a green-emitting QD displaying several copies of a yellow-fluorescing dye (e.g., Cy3 or Alexa Fluor 555, A555) and a second, redder acceptor dye (e.g., A647).[38] After specific photoexcitation of the QD, ET proceeds through three pathways: QD-to-A555 ($FRET_1$); A555-to-A647 ($FRET_2$), which occurs following the QD-to-A555 step; and QD-to-A647 ($FRET_3$). Although the first and last ET steps are in competition with one another; the initial QD-to-A555 step is far more efficient due to the more favorable underlying spectral overlap. As shown in Figure 3B, assembling differing ratios of both the A555 and A647 dyes to the initial QD donor results in a unique two-dimensional matrix of acceptor dye-to-QD PL ratios. When the biomolecular linkages attaching the acceptors to the QD are peptidyl protease substrates, two types of biosensors can be accessed. The first assays two unrelated or orthogonal reactions; assuming substrate independence (no cross-reactivity), the biosensor tracks the activity of two proteases, such as trypsin (TRP) and chymotrypsin (ChT), either individually or when comingled.[38] The second type of biosensor monitors linked enzymatic processes. For example, TRP activity and its activation of the inactive precursor pro-ChT to ChT can be tracked in real-time, as schematically shown in Figure 3C.

With cFRET, a single hybrid NP construct now effectively monitors two enzymatic (metabolic) reactions—either orthogonal or linked—with a single construct. From a materials standpoint, it is far simpler to utilize a single nanosensing construct and track changes in spectrally separated emissions than to implement two discrete nanosensors. Moreover, in both sensing formats, the ratiometric PL matrix provides a form of calibration curve that allows the observed changes in FRET ratios to be converted into quantitative units of enzymatic activity.[39] Analogous sensors utilizing DNA complementarity are equally viable.[40] The Algar Lab has taken the lead on exploring the biosensing space afforded by these sensors and has characterized protease sensing formats, DNA sensing formats, and mixed protease and DNA formats in solution as well as substrate-immobilized versions geared toward point-of-care (POC) applications.[41,42] Far more photophysically complex versions have incorporated time-gated FRET through the use of long-lifetime Tb chelates. Although both the QD and Tb chelate are initially excited, the chelate can still function as an initial donor to the QD following an appropriate time delay that allows the QD to relax back to the ground state. This configuration has been prototyped for both biosensing and molecular computing applications, with the latter providing unique access to time as a computational variable, allowing for the creation of repeated set−reset logic gates along with allowing "on-the-fly" gate transitions.[10,11,40]

DOI: 10.1021/acs.jpclett.6b00570
J. Phys. Chem. Lett. 2016, 7, 2139−2150

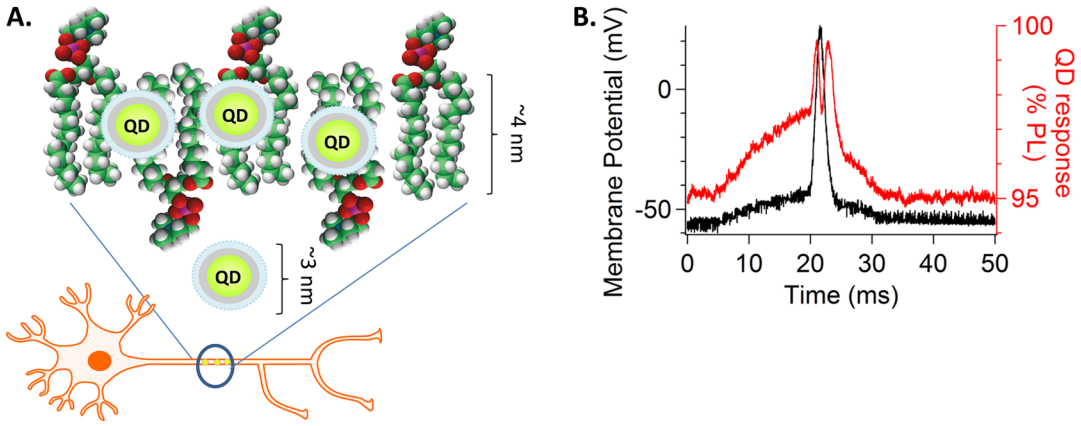

Figure 4. (A) Schematic suggesting that to be effective as voltage sensors, hydrophobic-surfaced QDs (~3 nm dia.) must be partitioned into the plasma membrane bilayer (~4 nm dia.) either physically or via liposomal delivery. (B) The QD PL response (red) must track temporally with the action potential spike (black). Note the two emission QD maxima at ~20−25 ms as the membrane potential proceeds twice through zero voltage. Panel B partially adapted from ref 51, copyright 2015 American Chemical Society.

Another fascinating opportunity for exploiting the unique interfacial properties of QDs is possible if these materials can be directly interfaced into the architecture of a neuronal plasma membrane. Nearly all cells, prokaryotes and eukaryotes alike, maintain a nonzero voltage or resting potential (ca. −40 to −80 mV) across their plasma membrane that is intimately tied to physiological processes aimed at maintaining cellular homeostasis.[43] Potential is maintained by transmembrane ion transporters/pumps and ion channels that preferentially move ions across the membrane. In excitable cells such as neurons and muscle cells, depolarization away from resting membrane potential results in transmission of nerve communication (in the form of action potentials) and muscle contraction, respectively. With such a pivotal role played by the membrane potential, it is surprising to note that many of the available tools to record or visualize electrical membrane activity (e.g., patch clamp, voltage-sensitive dyes) remain functionally quite limited.[44] With the inception of the BRAIN Initiative in 2013 came a renewed focus on developing functional nanomaterials with the requisite photophysical and electronic properties to probe the nanoscale expanse of the plasma membrane potential in ways not currently possible.[45] QDs have sparked considerable interest for this task given their brightness, photostability, energy/charge transfer capabilities, and large two-photon action cross sections.[6,46] Of particular interest is their quantum-confined Stark effect (QCSE) in response to an applied electric field (e-field), which is characterized by a decrease in QD PL (quenching) along with broadening and red-shifting of the QD emission spectra with increasing e-field strength.[47]

From a materials perspective, sufficient experimental and theoretical data exist to support the notion of using QDs as novel voltage-sensitive probes,[47,48] although a number of critical technical challenges remain. The first hurdle is the issue of QD size in the context of the ~4 nm thick aliphatic region of the plasma membrane (Figure 4A). To experience full e-field strength, the QD must be fully embedded (or screened) within this region as the e-field strength drops off exponentially within the 1 nm layer surrounding either side of the plasma membrane. This suggests that 3 nm diameter QDs may represent the upper size limit that can be inserted into the plasma membrane without perturbing membrane integrity.[49] As the QCSE scales with QD diameter (to the fourth power),[48] identifying appropriate QD materials/sizes that can be inserted into membranes, while providing the requisite optical responses, will be critical. Further considerations are the QD coating and the delivery method for partitioning the QD into the hydrophobic portion of the bilayer. The latter poses a significant challenge for carrying the QDs through aqueous cell culture media, although initial work with fusogenic unilamellar liposomal vesicles appears promising.[50] Finally, to be useful for voltage imaging, the QD PL response to the e-field must be on the millisecond or submillisecond time scale. Here, too, recent proof-of-concept work has shown that this is indeed achievable (Figure 4B).[51] Near-infrared-emitting gold nanoclusters may also have "potential" in this application, although their electrical and PL properties are not yet fully understood.[52]

Turning to the second overarching topic of this Perspective, beyond the effects of the nanoscale architecture, it is apparent that the localized interfacial environment found around these composite nanomaterials is both starkly different from the bulk solution environment and also largely uncharacterized.[17] This is conceptually highlighted in Figure 1, where the localized environment around the QD−enzyme conjugate is indicated and differentiated by the pink halo. In reality, the extent of how far from the NP surface this environment extends is still unknown. Nevertheless, similar to the first concept above, these phenomena present both challenges and new opportunities. Considering the physicochemical properties of nanobioconjugates, it is important first to account for ways in which the NP interacts with its surrounding environment. For example, organic solvents and water form structured layers around NPs due to hydrogen bonding between NP surface ligands, which serve to provide colloidal stability, and the immediately surrounding solvent molecules. Subsequent hydrogen bonding within successive layers of solvent molecules propagates the oriented structure, though less rigidly with each ensuing layer (Figure 5A). This has been considered, indirectly measured, and modeled for some time,[17] but only recently has it been directly observed for NPs.[53]

Organic ligands on the NP surface often display charged species to the surrounding media to confer colloidal stability by ionic stabilization as well as providing chemical handles for bioconjugation reactions. These ionic species confer a pH-dependent net charge to the particles. In addition to solvent restructuring at the NP surface, ions and counterions form a

DOI: 10.1021/acs.jpclett.6b00570
J. Phys. Chem. Lett. 2016, 7, 2139−2150

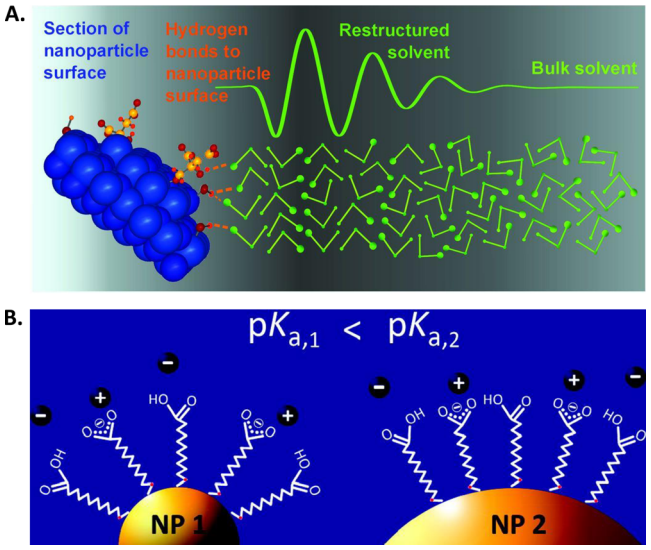

Figure 5. (A) Enhanced short-range order of solvent molecules at ZnO NP surfaces. The ethanol molecules (hydrogen atoms omitted) form hydrogen bonds with surface hydroxyl groups and citrate molecules. The surface coverage of these groups is reduced for means of clarity. The enhanced short-range order extends a few molecular layers into the bulk liquid before bulk properties are recovered. Figure reproduced from ref 53 with permission. Copyright 2015 AAAS. (B) Schematic illustrating how the dissociation of ionizable ligands displayed on NPs can be regulated by NP curvature. Reproduced from ref 55, copyright 2011 American Chemical Society.

Stern double layer to balance the surface charges exhibited by the inorganic NP and its associated ligands.[17] Fascinatingly, the aggregation of charges at a NP surface can have a dramatic impact on the physicochemical properties of the NP (and NP bioconjugate) and the chemical behavior of the organic ligand itself. For example, titration of carboxyl-functionalized NPs shows that the pK_a of the carboxylate is significantly higher for the NP coating than that for the free ligand.[54,55] The density of negative charges on the surface, which stabilizes the colloid through electrostatic repulsion, also undergoes charge−charge repulsion within the surface coating, or a kind of intraparticle electrostatic repulsion. This favors protonation of the carboxylates at much lower hydronium ion concentrations, resulting in NP-bound carboxylate pK_a values approximately 2−2.5 pH steps higher than those for the free carboxylates.[54,55] Moreover, these changes are dependent upon both NP size and curvature (Figure 5B). Changes in the pH of the media/solvent, in turn, change the surface charge (typically measured through a zeta potential) of electrostatically stabilized colloids as the ligands become protonated or deprotonated. Less surface charge reduces particle stability, increasing agglomeration. Hence a change in the pH of the NP solution may have the downstream effect of changing other physiochemical properties, such as the particle/cluster size, which can, in turn, impact characteristics such as the particle diffusion rate, S/V ratio, gross radius of curvature, and so forth. The take home message here is that in the specific context of a NP bioconjugate, these phenomena are not easily predicted or modeled. Additionally, research in this area is severely hampered by a lack of available metrologies capable of reporting with any fidelity on conditions in a nanoscale interface packed with organic ligands, ions, and biomolecules.[15] The interested reader is referred to an excellent review from the Parak Group discussing the nature of the NP interface and its influence.[17]

The influence of this altered environment on subsequent biomolecular activity occurring within it also remains uncharacterized; however, as recently shown, this may not be wholly detrimental. The most prevalent example to date of such beneficial properties is that of enzyme acceleration at a NP interface.[56−58] This phenomena appears to manifest when either the substrate or enzyme is attached to the NP surface, although it is not clear if the same underlying processes are responsible for the enhancements found within each configuration. Some of the contributing mechanisms behind this enhancement are more tractable to dissection using the substrate-on-NP format rather than that of the converse configuration. For example, utilizing acceptor dye-labeled peptidyl substrates displayed around central QD donors, Algar, et al., were able to quantitatively monitor the kinetic efficiency of the protease trypsin acting upon this multivalent NP−substrate.[39] Achieving a conventional excess-substrate format with this configuration is not possible due to QD concentration limits (high μM to mM concentrations of QDs in buffer are not a physical reality), and these experiments necessitated a slightly more complex progress curve format (i.e., fixed substrate, excess enzyme) assayed over longer time periods to collect suitable data (Figure 6A). The use of an integrated Michaelis−Menten analysis in conjunction with kinetic modeling suggested a "hopping" mode of catalysis, whereby TRP interacts with a single QD and cleaves all of the substrate displayed around it before diffusing away to the next encounter (Figure 6B). TRP cleavage efficiency was effectively enhanced up to 5-fold in this configuration compared to controls containing the equivalent concentration of freely

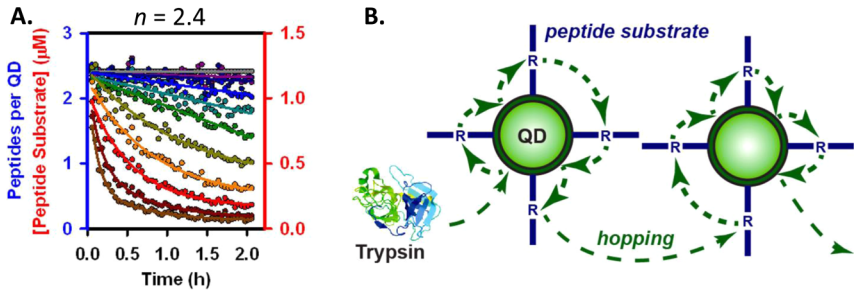

Figure 6. (A) Progress curve tracking TRP digestion of QD−peptide substrates. QDs were conjugated with an average of 2.4 peptides each. The different colors represent different concentrations of TRP ranging from 0 to 343 nM. (B) Model of a "hopping" mechanism of enzyme activity whereby an individual TRP molecule encounters a QD−substrate complex and consumes all of the attached substrate before diffusing away to the next encounter. Reproduced from ref 39, copyright 2012 American Chemical Society.

DOI: 10.1021/acs.jpclett.6b00570
J. Phys. Chem. Lett. 2016, 7, 2139−2150

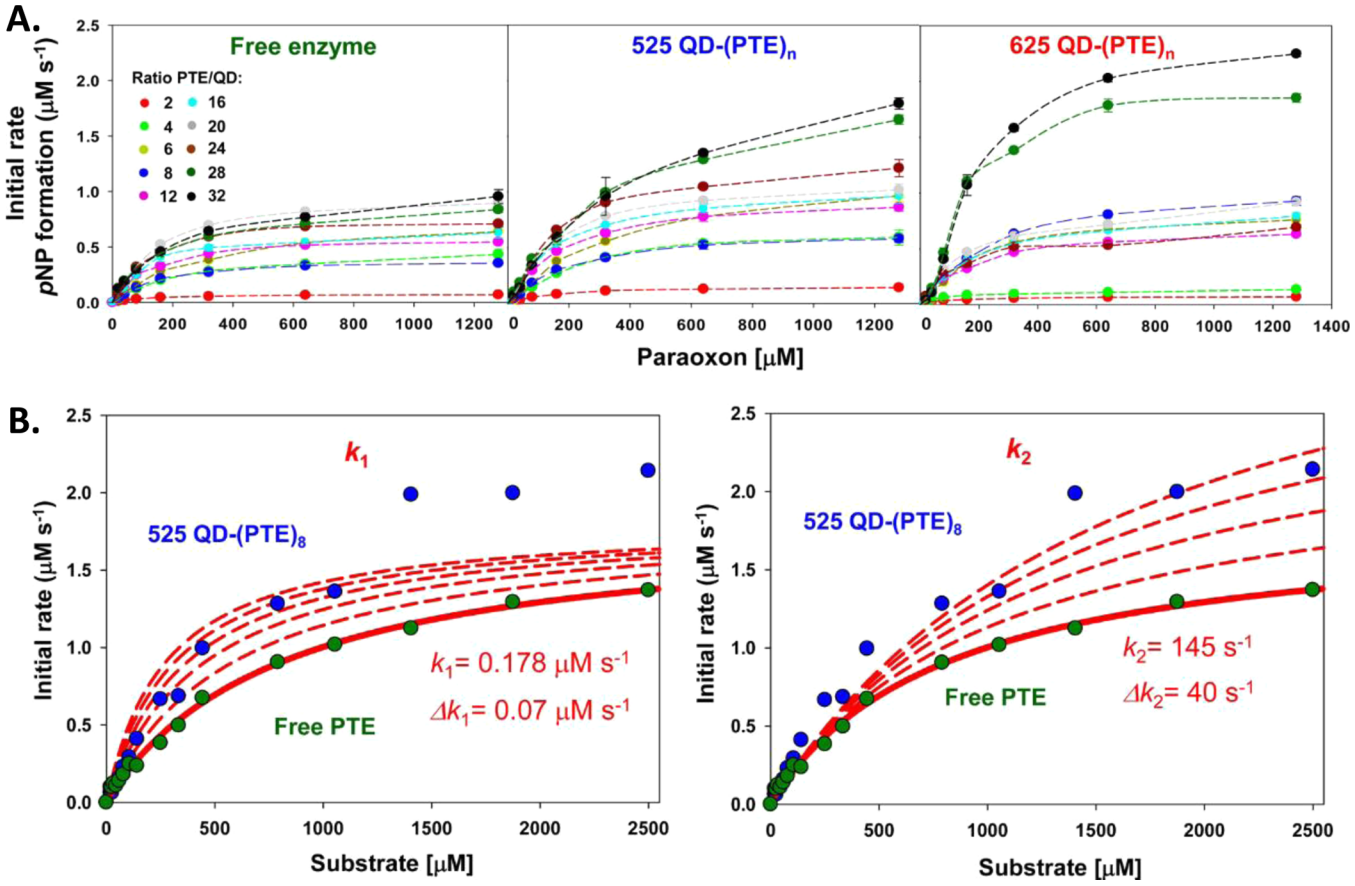

Figure 7. (A) QD−PTE bioconjugate activity. Initial rates of product formation for free PTE (left), 525 QD−$(PTE)_n$ (middle), and 625 QD−$(PTE)_n$ (right) bioconjugates assembled at the indicated ratios when exposed to an increasing concentration of paraoxon substrate. The free PTE enzyme is at the equivalent concentration as that used for the QD bioconjugates. (B) Plot comparing the effect of potential changes in k_1 (enzyme−substrate association) and k_2 (enzyme−product disassociation) on initial PTE rates. The experimental rates of free PTE (green) and 525 QD−$(PTE)_8$ (blue) versus substrate concentration are plotted. The red lines plot the effect of an increase in either k_1 or k_2 on the initial PTE activity. Reproduced from ref 60, copyright 2015 American Chemical Society.

diffusing enzyme and substrate. Similar to the previous examples, enhancement of TRP activity can be partially ascribed to the unique nanobioconjugate architecture. Because multiple substrates are displayed on a NP with very high avidity, the enzyme may be more favored to interact with another substrate than randomly diffusing away.

The physicochemical environment found at this QD−substrate−enzyme interface will clearly play a strong role in dictating how TRP, in this case, interacts with the peptidyl substrate displayed around the QD. Although the initial encounter may be based on random diffusion, the NP surface ligands can act to either electrostatically attract or repulse the enzyme, depending on the net charge that each displays to the other. It is easy to hypothesize that increased enzyme dwell times when encountering this NP, along with a relatively fixed and preferred substrate orientation, can synergistically induce the enzyme to rapidly consume its way around the QD−substrate, yielding an increase in the localized catalytic rate. Similarly structured QD−substrate assemblies, albeit with different QD ligands and proteases, exhibited decreased enzymatic activity, presumably due to nonoptimal interactions at the QD−substrate−enzyme interface.[59] The confounding issue is that because the true localized environment around the NP (e.g., pH, pK_a, ligand density, ion concentrations, etc.) is not easily determined, it is extremely challenging to establish a predictive framework for even the simplest types of biocatalytic activity seen with these materials, such as a "hopping" mode of catalysis.

Enzymatic activity enhancement has also been observed in the converse configuration, where enzymes are displayed around a NP. A recent study utilizing QDs displaying phosphotriesterase (PTE) provided critical insight into how enzyme activity is mechanistically altered by the localized microenvironment.[60] PTE is capable of hydrolyzing organophosphate ester compounds, making it of focused interest for nerve agent decontamination.[61] Figure 7A shows representative plots of activity from increasing concentrations of PTE when freely diffusing and when displayed on 525 and 625 nm emitting QDs (diameters of ∼4.2 and ∼9.2 nm, respectively). The significant increase in the QD-conjugated enzyme's initial rate of paraoxon substrate conversion to *p*-nitrophenol product (*p*NP) is readily apparent here with a 4-fold increase in initial rate and a 2-fold improvement in enzymatic efficiency. A detailed kinetic analysis of this conjugate showed no change in substrate specificity or in the activation energy between freely diffusing and QD-bound PTE. Rather, experimental results and kinetic modeling of this experimental data suggested that the improved activity results from an acceleration in enzyme−product dissociation. The Raushel Group's foundational work with PTE showed that its rate-limiting step is enzyme−product dissociation, as represented using the following slightly expanded Michaelis−Menten expression[61]

DOI: 10.1021/acs.jpclett.6b00570
J. Phys. Chem. Lett. 2016, 7, 2139−2150

$$\overbrace{\mathrm{E} + \mathrm{S} \underset{k_{-1}}{\overset{k_1}{\rightleftarrows}} \mathrm{ES}}^{\text{Step 1}} \overbrace{\xrightarrow{k_{\mathrm{cat}}^{\mathrm{R}}} \mathrm{EP}}^{\text{Step 2}} \overbrace{\underset{k_{-2}}{\overset{k_2}{\rightleftarrows}} \mathrm{E} + \mathrm{P}}^{\text{Step 3}} \quad (2)$$

Here E, S, P, ES, and EP represent the enzyme, substrate, product, enzyme−substrate complex, and enzyme−product complex, respectively, and k_n are the various association/dissociation constants. $k_{\mathrm{cat}}^{\mathrm{R}}$ differs from the traditional k_{cat} in that it stipulates only the catalytic turnover rate (hydrolysis) and not also EP dissociation implicitly, as is more common. Thus, PTE activity consists of three distinct physical steps or stages: (1) ES formation as governed by k_1, (2) catalytic hydrolysis, and (3) EP dissociation as governed by k_2, the measured rate-limiting step.[61,62] Figure 7B shows the results of kinetic modeling using experimentally derived data where the difference between the activity of free PTE and QD-conjugated PTE is accounted for by attempting stepwise increases to either k_1 or k_2. The qualitatively better fit between free and QD-conjugated experimental formats becomes readily apparent when changing k_2. Barring an increase in k_1, the other possible enhancement mechanism would be a significant improvement in enzyme−substrate affinity or K_{M}; however, the experimental data showed that this actually decreased slightly when the enzyme was displayed on the QD.

These systems are extremely hard to study as it is nearly impossible to isolate single variables among the complexity.

Therefore, why would k_2 or the EP dissociation rate change, and so favorably at that? It presumably originates from the markedly different microenvironment found within the PTE−QD bioconjugate's hydration layer. Similar NP−enzyme conjugate enhancement results have been observed when attaching a trimeric PTE or alkaline phosphatase to QDs.[63,64] Enzymatic enhancements have also been observed when displaying the QDs around an even larger tetrameric β-galactosidase enzyme complex (~465 kDa).[65] It is estimated that there are now >200 reported examples of some type of activity enhancement when enzymes are attached to NPs,[56−58] but there remains still no consensus on the mechanics underlying this phenomenon. Indeed, a variety of factors have been suggested, including NP shielding effects, improvements to K_{M}, improved enzyme conformation, localized substrate confinement or capture, and improved substrate trajectories. It is not clear if this diversity in proposed mechanisms is physical or just reflective of our poor understanding of NP−enzyme enhancement and the NP interface in general. Even without achieving this understanding, these high-affinity NP−substrate conjugates may still serve as powerful research platforms for developing downstream opportunities like NP-mediated drug delivery (NMDD).[9,66,67] Most drug targets are enzymes, and in the context of theranostics, NMDD seeks to create platforms for specifically delivering and targeting highly toxic or poorly soluble drug compounds in a high-avidity construct. This is meant to circumvent issues associated with the generalized, systemic delivery of therapeutics. Clearly, a basic understanding of the localized environment and kinetics of enzyme activity at this interface will be critical to this endeavor. NP−enzyme conjugates themselves may present other opportunities. Due to their metastable character and the need for sample cleanup in a process stream, enzymes have long been attached to microparticles for use in industrial catalysis. Although this can stabilize the enzymes and facilitate their removal from a reaction, heterogeneous attachment to these essentially localized planar surfaces usually decreases enzyme activity.[68,69] NP−enzyme constructs and related structures not only display increased activity but also exhibit improved long-term stability.[70] It is not out of the realm of possibility to envision NP−enzyme constructs being utilized as nanoscale therapeutics to treat enzyme deficiencies or other medical ailments that would benefit from a catalytic reaction, such as rendering a toxin inert.[66,67]

In addition to affecting the activity of enzymes, NPs directly engage and interact with proteins differently as well. The many ways that proteinaceous molecules, ranging from short

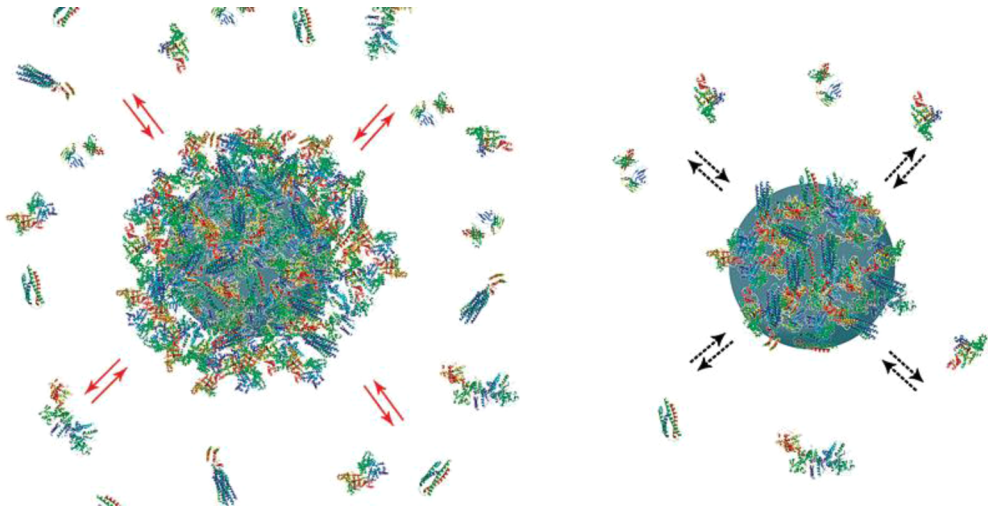

Figure 8. In plasma, NPs are surrounded by a corona of proteins. In situ (left), a weakly interacting protein outer layer rapidly exchanges with proteins in the plasma. When the complexes are isolated from plasma and carefully washed (right), only a slowly exchanging "hard" corona of proteins with sufficiently long residence times remains, highlighting the dynamic and concentration/affinity-driven nature of the protein interaction with the NPs over time. Reproduced from ref 77, copyright 2010 American Chemical Society.

DOI: 10.1021/acs.jpclett.6b00570
J. Phys. Chem. Lett. 2016, 7, 2139−2150

polypeptides to large antibodies, can physicochemically interact with and attach to NPs is well beyond the scope of this Perspective but has been discussed in multiple reviews.[15,18−20] More relevant here are how undirected proteins interact with a NP surface and how those interactions change the nature of the NP presentation to its surroundings; this is commonly referred to as the protein corona.[21,22,71−73] Put another way, the nonspecific interactions between proteins and NPs alter the surface that is displayed to the surrounding media, meaning that these very interactions change the physical chemistry of the NPs. It is not just proteins that interact with NPs but all manner of (bio)molecules ranging from ions and solutes to membranes, nucleic acids, and lipids.[21,22,71−73] Much of our understanding of this topic originates with the long history of studies into interactions between macroscopic biomaterials and the proteins found in physiologic fluids, but this dynamic is changed in subtle and important ways when the material (i.e., the NP) and the protein approach the same size scale. As succinctly stated by Chan, "When a NP [*sic* nanomaterial] enters a physiological environment, its surface is immediately covered by a layer of proteins, forming what is known as the protein 'corona'. The protein corona alters the size, aggregation state, and interfacial properties of the NP [*sic* nanomaterial], giving it a biological identity that is distinct from its synthetic identity."[71] Moreover, the corona on a NP in serum or blood, for example, appears to be a very dynamic system with the initially formed display of high-abundance/low-affinity proteins exchanging for low-abundance/high-affinity proteins over time (Figure 8).[21,22,71−73] The complexity of these systems will be significantly exacerbated when the NPs are biofunctionalized and/or subsequently interact with cells or other complex bioenvironments.

These systems are extremely hard to study as it is nearly impossible to isolate single variables among the complexity. A particularly innovative approach to overcome this issue from the Parak Group isolated the surface charge variable from pH-dependent protonation states or other aspects of coating-dependent colloidal stability, yielding rare insight into the impact of an isolated physiochemical variable.[74] Here, AuNPs coated with amphiphilic polymers displayed persistent negative and positive charges via phosphonate and trimethylammonium polar groups, respectively. This pH-insensitive surface chemistry stands in contrast to the typical carboxyl and amine functionalities found on ligands, which are protonated and deprotonated at relevant pHs, confounding direct correlations between charge, pH, and properties like colloidal stability or protein adsorption. With this approach, they found that the number of adsorbed human serum albumin molecules per NP was not influenced by the NP surface charge and positively charged NPs were incorporated by cells to a larger extent than negatively charged ones, both in serum-free and serum-containing media. These somewhat unexpected findings suggest the presence of influential material characteristics beyond surface charge that likely exhibit both complex, interrelated interactions with the environment and individual unrelated activities. Clearly, protein corona formation and its subsequent dynamics will not easily lend themselves to dissection and analysis. Although concerted progress is being made, this vexing issue joins others such as NP toxicity that still lack an easily attainable predictive framework.[74,78]

Although a comprehensive understanding of the specific design elements governing both protein corona formation and the subsequent long-term properties of the bioconjugated material is still distant, applications exploiting these dynamic interactions are already on the horizon. For example, the protein corona may act to stealthily disguise NP-based therapeutics in vivo to avoid unwanted recognition, interactions, or clearance while protecting any "cargo" attached to the NP.[75] A dynamic corona exchange in situ could then reveal a targeting moiety, such as an aptamer, along with a drug or sensor at a specific time or in response to a specific biomolecular signal.

Positive device attributes and new application potential may arise from the extremely complicated or even unpredictable physicochemical phenomena that occur at the NP−biomolecular interface.

In summary, the complexities inherent to the localized NP environment are amplified when biomolecules are added to the system, either concertedly through bioconjugation or in an undirected manner via the protein corona. Although only a partial subset of available nanomaterials are used here to illustrate the pertinent concepts, we expect these phenomena to hold true across a wide swath of materials including both hard and soft NPs of quite diverse composition. Clearly, the structural and physiochemical properties of nanomaterial−biomolecular conjugates provide a yin and yang-like set of opportunities and caveats that must be considered when designing such hybrid devices. In this Perspective, we suggest that positive device attributes and new application potential may arise from the extremely complicated or even unpredictable physicochemical phenomena that occur at the NP−biomolecular interface. Far more examples, beyond those discussed here, are sure to appear in the near future as the various projected applications for NP bioconjugates transition from concept to research to actual utility.

AUTHOR INFORMATION

Corresponding Author

*E-mail: Igor.medintz@nrl.navy.mil.

Notes

The authors declare no competing financial interest.

Biographies

Prof. Allison Dennis earned her Ph.D. in Bioengineering from the Georgia Institute of Technology. She has been an Assistant Professor of Biomedical Engineering and Materials Science and Engineering at Boston University since 2013. Her research focuses on advanced quantum dot chemistries for biosensing and biomedical imaging applications (http://sites.bu.edu/dennislab/).

Dr. James Delehanty received his Ph.D. in Molecular and Cellular Biology from Tulane University Health Sciences Center. He is currently a research biologist in the Center for Bio/Molecular Science and Engineering at the U.S. Naval Research Laboratory. His research focuses on the interfacing of a variety of NP bioconjugates with cells for imaging, sensing, and cargo delivery applications.

Dr. Igor Medintz received his Ph.D. in Molecular and Cellular Biology from the City University of New York in 1999. He is at the Center for Bio/Molecular Science and Engineering at the U.S. Naval Research

DOI: 10.1021/acs.jpclett.6b00570
J. Phys. Chem. Lett. 2016, 7, 2139−2150

Laboratory where he is the Navy's Senior Scientist for Biosensors and Biomaterials. His research focuses on understanding biological activity at nanomaterial interfaces and how nanomaterials and biologicals engage in energy transfer.

■ ACKNOWLEDGMENTS

I.M. and J.B.D. acknowledge the NRL Nanosciences Institute and DTRA JSTO MIPR #B112582M. A.M.D. acknowledges support from the NSF under Grant No. CBET 1505718.

■ REFERENCES

(1) Jirgensons, B.; Straumanis, M. R. E. *A Short Textbook of Colloid Chemistry*, 2nd Ed.; Macmillan: New York, 1962.
(2) Faulk, W. P.; Taylor, G. M. Immunocolloid Method for Electron Microscope. *Immunochemistry* **1971**, *8*, 1081−1083.
(3) Tonga, G. Y.; Saha, K.; Rotello, V. M. 25th Anniversary Article: Interfacing Nanoparticles and Biology: New Strategies for Biomedicine. *Adv. Mater.* **2014**, *26*, 359−370.
(4) Wagner, N. L.; Greco, J. A.; Ranaghan, M. J.; Birge, R. R. Directed Evolution of Bacteriorhodopsin for Applications in Bioelectronics. *J. R. Soc., Interface* **2013**, *10*, 20130197.
(5) Sapsford, K. E.; Algar, W. R.; Berti, L.; Gemmill, K. B.; Casey, B. J.; Oh, E.; Stewart, M. H.; Medintz, I. L. Functionalizing Nanoparticles with Biological Molecules: Developing Chemistries That Facilitate Nanotechnology. *Chem. Rev.* **2013**, *113*, 1904−2074.
(6) Wegner, K. D.; Hildebrandt, N. Quantum Dots: Bright and Versatile in Vitro and in Vivo Fluorescence Imaging Biosensors. *Chem. Soc. Rev.* **2015**, *44*, 4792−4834.
(7) Daniel, M. C.; Astruc, D. Gold Nanoparticles: Assembly, Supramolecular Chemistry, Quantum-Size-Related Properties, and Applications toward Biology, Catalysis, and Nanotechnology. *Chem. Rev.* **2004**, *104*, 293−346.
(8) Lux Research Inc. *Nanotechnology Update: Corporations Up Their Spending as Revenues for Nano-Enabled Products Increase*; Boston, MA, 2014.
(9) Delehanty, J. B.; Boeneman, K.; Bradburne, C. E.; Robertson, K.; Medintz, I. L. Quantum Dots: A Powerful Tool for Understanding the Intricacies of Nanoparticle-Mediated Drug Delivery. *Expert Opin. Drug Delivery* **2009**, *6*, 1091−1112.
(10) Claussen, J. C.; Algar, W. R.; Hildebrandt, N.; Susumu, K.; Ancona, M. G.; Medintz, I. L. Biophotonic Logic Devices Based on Quantum Dots and Temporally-Staggered Forster Energy Transfer Relays. *Nanoscale* **2013**, *5*, 12156−12170.
(11) Claussen, J. C.; Hildebrandt, N.; Susumu, K.; Ancona, M. G.; Medintz, I. L. Complex Logic Functions Implemented with Quantum Dot Bionanophotonic Circuits. *ACS Appl. Mater. Interfaces* **2014**, *6*, 3771−3778.
(12) Mariano, M.; El Kissi, N.; Dufresne, A. Cellulose Nanocrystals and Related Nanocomposites: Review of Some Properties and Challenges. *J. Polym. Sci., Part B: Polym. Phys.* **2014**, *52*, 791−806.
(13) Yang, W. R.; Thordarson, P.; Gooding, J. J.; Ringer, S. P.; Braet, F. Carbon Nanotubes for Biological and Biomedical Applications. *Nanotechnology* **2007**, *18*, 412001.
(14) Samanta, A.; Medintz, I. L. Nanoparticles and DNA − A Powerful and Growing Functional Combination in Bionanotechnology. *Nanoscale* **2016**, *8*, 9037.
(15) Sapsford, K. E.; Tyner, K. M.; Dair, B. J.; Deschamps, J. R.; Medintz, I. L. Analyzing Nanomaterial Bioconjugates: A Review of Current and Emerging Purification and Characterization Techniques. *Anal. Chem.* **2011**, *83*, 4453−4488.
(16) Gonzalez Solveyra, E.; Szleifer, I. What Is the Role of Curvature on the Properties of Nanomaterials for Biomedical Applications? *WIREs Nanomed. Nanobiotech.* **2016**, *8*, 334−354.
(17) Pfeiffer, C.; Rehbock, C.; Huhn, D.; Carrillo-Carrion, C.; de Aberasturi, D. J.; Merk, V.; Barcikowski, S.; Parak, W. J. Interaction of Colloidal Nanoparticles with Their Local Environment: The (Ionic) Nanoenvironment around Nanoparticles Is Different from Bulk and Determines the Physico-Chemical Properties of the Nanoparticles. *J. R. Soc., Interface* **2014**, *11*, 20130931.
(18) Algar, W. R.; Prasuhn, D. E.; Stewart, M. H.; Jennings, T. L.; Blanco-Canosa, J. B.; Dawson, P. E.; Medintz, I. L. The Controlled Display of Biomolecules on Nanoparticles: A Challenge Suited to Bioorthogonal Chemistry. *Bioconjugate Chem.* **2011**, *22*, 825−858.
(19) Biju, V. Chemical Modifications and Bioconjugate Reactions of Nanomaterials for Sensing, Imaging, Drug Delivery and Therapy. *Chem. Soc. Rev.* **2014**, *43*, 744−764.
(20) Medintz, I. Universal Tools for Biomolecular Attachment to Surfaces. *Nat. Mater.* **2006**, *5*, 842−842.
(21) Foroozandeh, P.; Aziz, A. A. Merging Worlds of Nanomaterials and Biological Environment: Factors Governing Protein Corona Formation on Nanoparticles and Its Biological Consequences. *Nanoscale Res. Lett.* **2015**, *10*, 221.
(22) Moore, T. L.; Rodriguez-Lorenzo, L.; Hirsch, V.; Balog, S.; Urban, D.; Jud, C.; Rothen-Rutishauser, B.; Lattuada, M.; Petri-Fink, A. Nanoparticle Colloidal Stability in Cell Culture Media and Impact on Cellular Interactions. *Chem. Soc. Rev.* **2015**, *44*, 6287−6305.
(23) Mammen, M.; Choi, S. K.; Whitesides, G. M. Polyvalent Interactions in Biological Systems: Implications for Design and Use of Multivalent Ligands and Inhibitors. *Angew. Chem., Int. Ed.* **1998**, *37*, 2754−2794.
(24) Raita, M.; Arnthong, J.; Champreda, V.; Laosiripojana, N. Modification of Magnetic Nanoparticle Lipase Designs for Biodiesel Production from Palm Oil. *Fuel Process. Technol.* **2015**, *134*, 189−197.
(25) Haller, E.; Lindner, W.; Lammerhofer, M. Gold Nanoparticle-Antibody Conjugates for Specific Extraction and Subsequent Analysis by Liquid Chromatography-Tandem Mass Spectrometry of Malondialdehyde-Modified Low Density Lipoprotein as Biomarker for Cardiovascular Risk. *Anal. Chim. Acta* **2015**, *857*, 53−63.
(26) Pinaud, F.; Clarke, S.; Sittner, A.; Dahan, M. Probing Cellular Events, One Quantum Dot at a Time. *Nat. Methods* **2010**, *7*, 275−285.
(27) Saxton, M. J.; Jacobson, K. Single-Particle Tracking: Applications to Membrane Dynamics. *Annu. Rev. Biophys. Biomol. Struct.* **1997**, *26*, 373−399.
(28) Lee, G. M.; Ishihara, A.; Jacobson, K. A. Direct Observation of Brownian-Motion of Lipids in a Membrane. *Proc. Natl. Acad. Sci. U. S. A.* **1991**, *88*, 6274−6278.
(29) Farlow, J.; Seo, D.; Broaders, K. E.; Taylor, M. J.; Gartner, Z. J.; Jun, Y. W. Formation of Targeted Monovalent Quantum Dots by Steric Exclusion. *Nat. Methods* **2013**, *10*, 1203−1205.
(30) Rosi, N. L.; Mirkin, C. A. Nanostructures in Biodiagnostics. *Chem. Rev.* **2005**, *105*, 1547−1562.
(31) Prigodich, A. E.; Alhasan, A. H.; Mirkin, C. A. Selective Enhancement of Nucleases by Polyvalent DNA-Functionalized Gold Nanoparticles. *J. Am. Chem. Soc.* **2011**, *133*, 2120−2123.
(32) Bi, S.; Dong, Y.; Jia, X. Q.; Chen, M.; Zhong, H.; Ji, B. Self-Assembled Multifunctional DNA Nanospheres for Biosensing and Drug Delivery into Specific Target Cells. *Nanoscale* **2015**, *7*, 7361−7367.
(33) Delyagina, E.; Schade, A.; Scharfenberg, D.; Skorska, A.; Lux, C.; Li, W. Z.; Steinhoff, G. Improved Transfection in Human Mesenchymal Stem Cells: Effective Intracellular Release of Pdna by Magnetic Polyplexes. *Nanomedicine* **2014**, *9*, 999−1017.
(34) Algar, W. R.; Kim, H.; Medintz, I. L.; Hildebrandt, N. Emerging Non-Traditional Forster Resonance Energy Transfer Configurations with Semiconductor Quantum Dots: Investigations and Applications. *Coord. Chem. Rev.* **2014**, *263-264*, 65−85.
(35) Medintz, I. L.; Hildebrandt, N. *FRET - Förster Resonance Energy Transfer. From Theory to Applications*; Wiley-VCH: Weinheim, Germany, 2014; pp 105−164.
(36) Chou, K. F.; Dennis, A. M. Förster Resonance Energy Transfer between Quantum Dot Donors and Quantum Dot Acceptors. *Sensors* **2015**, *15*, 13288−13325.
(37) Pons, T.; Medintz, I. L.; Wang, X.; English, D. S.; Mattoussi, H. Solution-Phase Single Quantum Dot Fluorescence Resonance Energy Transfer. *J. Am. Chem. Soc.* **2006**, *128*, 15324−15331.

DOI: 10.1021/acs.jpclett.6b00570
J. Phys. Chem. Lett. 2016, 7, 2139−2150

(38) Algar, W. R.; Ancona, M. G.; Malanoski, A. P.; Susumu, K.; Medintz, I. L. Assembly of a Concentric Forster Resonance Energy Transfer Relay on a Quantum Dot Scaffold: Characterization and Application to Multiplexed Protease Sensing. *ACS Nano* **2012**, *6*, 11044−11058.
(39) Algar, W. R.; Malonoski, A.; Deschamps, J. R.; Blanco-Canosa, J. B.; Susumu, K.; Stewart, M. H.; Johnson, B. J.; Dawson, P. E.; Medintz, I. L. Proteolytic Activity at Quantum Dot-Conjugates: Kinetic Analysis Reveals Enhanced Enzyme Activity and Localized Interfacial "Hopping". *Nano Lett.* **2012**, *12*, 3793−3802.
(40) Algar, W. R.; Wegner, D.; Huston, A. L.; Blanco-Canosa, J. B.; Stewart, M. H.; Armstrong, A.; Dawson, P. E.; Hildebrandt, N.; Medintz, I. L. Quantum Dots as Simultaneous Acceptors and Donors in Time-Gated Forster Resonance Energy Transfer Relays: Characterization and Biosensing. *J. Am. Chem. Soc.* **2012**, *134*, 1876−1891.
(41) Petryayeva, E.; Algar, W. R. Toward Point-of-Care Diagnostics with Consumer Electronic Devices: The Expanding Role of Nanoparticles. *RSC Adv.* **2015**, *5*, 22256−22282.
(42) Wu, M.; Petryayeva, E.; Algar, W. R. Quantum Dot-Based Concentric Fret Configuration for the Parallel Detection of Protease Activity and Concentration. *Anal. Chem.* **2014**, *86*, 11181−11188.
(43) Yang, M.; Brackenbury, W. J. Membrane Potential and Cancer Progression. *Front. Physiol.* **2013**, *4*, 185.
(44) Peterka, D. S.; Takahashi, H.; Yuste, R. Imaging Voltage in Neurons. *Neuron* **2011**, *69*, 9−21.
(45) Alivisatos, A. P.; et al. Nanotools for Neuroscience and Brain Activity Mapping. *ACS Nano* **2013**, *7*, 1850−1866.
(46) Andrasfalvy, B. K.; Galinanes, G. L.; Huber, D.; Barbic, M.; Macklin, J. J.; Susumu, K.; Delehanty, J. B.; Huston, A. L.; Makara, J. K.; Medintz, I. L. Quantum Dot-Based Multiphoton Fluorescent Pipettes for Targeted Neuronal Electrophysiology. *Nat. Methods* **2014**, *11*, 1237−1241.
(47) Park, K.; Deutsch, Z.; Li, J. J.; Oron, D.; Weiss, S. Single Molecule Quantum-Confined Stark Effect Measurements of Semiconductor Nanoparticles at Room Temperature. *ACS Nano* **2012**, *6*, 10013−10023.
(48) Marshall, J. D.; Schnitzer, M. J. Optical Strategies for Sensing Neuronal Voltage Using Quantum Dots and Other Semiconductor Nanocrystals. *ACS Nano* **2013**, *7*, 4601−9.
(49) Zheng, W.; Liu, Y.; West, A.; Schuler, E. E.; Yehl, K.; Dyer, R. B.; Kindt, J. T.; Salaita, K. Quantum Dots Encapsulated within Phospholipid Membranes: Phase-Dependent Structure, Photostability, and Site-Selective Functionalization. *J. Am. Chem. Soc.* **2014**, *136*, 1992−9.
(50) Gopalakrishnan, G.; Danelon, C.; Izewska, P.; Prummer, M.; Bolinger, P. Y.; Geissbuhler, I.; Demurtas, D.; Dubochet, J.; Vogel, H. Multifunctional Lipid/Quantum Dot Hybrid Nanocontainers for Controlled Targeting of Live Cells. *Angew. Chem., Int. Ed.* **2006**, *45*, 5478−5483.
(51) Rowland, C. E.; et al. Electric Field Modulation of Semiconductor Quantum Dot Photoluminescence: Insights into the Design of Robust Voltage-Sensitive Cellular Imaging Probes. *Nano Lett.* **2015**, *15*, 6848−6854.
(52) Oh, E.; et al. Pegylated Luminescent Gold Nanoclusters: Synthesis, Characterization, Bioconjugation, and Application to One- and Two-Photon Cellular Imaging. *Part. Part. Syst. Charact.* **2013**, *30*, 453−466.
(53) Zobel, M.; Neder, R. B.; Kimber, S. A. J. Universal Solvent Restructuring Induced by Colloidal Nanoparticles. *Science* **2015**, *347*, 292−294.
(54) Charron, G.; Huhn, D.; Perrier, A.; Cordier, L.; Pickett, C. J.; Nann, T.; Parak, W. J. On the Use of pH Titration to Quantitatively Characterize Colloidal Nanoparticles. *Langmuir* **2012**, *28*, 15141−15149.
(55) Wang, D. W.; Nap, R. J.; Lagzi, I.; Kowalczyk, B.; Han, S. B.; Grzybowski, B. A.; Szleifer, I. How and Why Nanoparticle's Curvature Regulates the Apparent pKa of the Coating Ligands. *J. Am. Chem. Soc.* **2011**, *133*, 2192−2197.
(56) Johnson, B. J.; Algar, W. R.; Malanoski, A. P.; Ancona, M. G.; Medintz, I. L. Understanding Enzymatic Acceleration at Nanoparticle Interfaces: Approaches and Challenges. *Nano Today* **2014**, *9*, 102−131.
(57) Ansari, S. A.; Husain, Q. Potential Applications of Enzymes Immobilized on/in Nano Materials: A Review. *Biotechnol. Adv.* **2012**, *30*, 512−523.
(58) Ding, S. W.; Cargill, A. A.; Medintz, I. L.; Claussen, J. C. Increasing the Activity of Immobilized Enzymes with Nanoparticle Conjugation. *Curr. Opin. Biotechnol.* **2015**, *34*, 242−250.
(59) Diaz, S. A.; Malonoski, A. P.; Susumu, K.; Hofele, R. V.; Oh, E.; Medintz, I. L. Probing the Kinetics of Quantum Dot-Based Proteolytic Sensors. *Anal. Bioanal. Chem.* **2015**, *407*, 7307−7318.
(60) Breger, J. C.; Ancona, M. G.; Walper, S. A.; Oh, E.; Susumu, K.; Stewart, M. H.; Deschamps, J. R.; Medintz, I. L. Understanding How Nanoparticle Attachment Enhances Phosphotriesterase Kinetic Efficiency. *ACS Nano* **2015**, *9*, 8491−8503.
(61) Tsai, P. C.; Fox, N.; Bigley, A. N.; Harvey, S. P.; Barondeau, D. P.; Raushel, F. M. Enzymes for the Homeland Defense: Optimizing Phosphotriesterase for the Hydrolysis of Organophosphate Nerve Agents. *Biochemistry* **2012**, *51*, 6463−6475.
(62) Bigley, A. N.; Raushel, F. M. Catalytic Mechanisms for Phosphotriesterases. *Biochim. Biophys. Acta, Proteins Proteomics* **2013**, *1834*, 443−453.
(63) Breger, J. C.; Walper, S. A.; Oh, E.; Susumu, K.; Stewart, M. H.; Deschamps, J. R.; Medintz, I. L. Quantum Dot Display Enhances Activity of a Phosphotriesterase Trimer. *Chem. Commun.* **2015**, *51*, 6403−6406.
(64) Claussen, J. C.; Malanoski, A.; Breger, J. C.; Oh, E.; Walper, S. A.; Susumu, K.; Goswami, R.; Deschamps, J. R.; Medintz, I. L. Probing the Enzymatic Activity of Alkaline Phosphatase within Quantum Dot Bioconjugates. *J. Phys. Chem. C* **2015**, *119*, 2208−2221.
(65) Brown, C. W., III; Oh, E.; Hastman, D. A. J.; Walper, S. A.; Susumu, K.; Stewart, M. H.; Deschamps, J. R.; Medintz, I. L. Kinetic Enhancement of the Diffusion-Limited Enzyme Beta-Galactosidase When Displayed with Quantum Dots. *RSC Adv.* **2015**, *5*, 93089−93094.
(66) Min, Y. Z.; Caster, J. M.; Eblan, M. J.; Wang, A. Z. Clinical Translation of Nanomedicine. *Chem. Rev.* **2015**, *115*, 11147−11190.
(67) Tong, R.; Kohane, D. S. New Strategies in Cancer Nanomedicine. *Annu. Rev. Pharmacol. Toxicol.* **2016**, *56*, 41−57.
(68) Feng, X. D.; Li, C. The Improvement of Enzyme Properties and Its Catalytic Engineering Strategy. *Progress Chem.* **2015**, *27*, 1649−1657.
(69) Liu, Y. S.; Yu, J. Oriented Immobilization of Proteins on Solid Supports for Use in Biosensors and Biochips: A Review. *Microchim. Acta* **2016**, *183*, 1−19.
(70) Alves, N. J.; Turner, K. B.; Daniele, M. A.; Oh, E.; Medintz, I. L.; Walper, S. A. Bacterial Nanobioreactors-Directing Enzyme Packaging into Bacterial Outer Membrane Vesicles. *ACS Appl. Mater. Interfaces* **2015**, *7*, 24963−24972.
(71) Walkey, C. D.; Chan, W. C. Understanding and Controlling the Interaction of Nanomaterials with Proteins in a Physiological Environment. *Chem. Soc. Rev.* **2012**, *41*, 2780−2799.
(72) Corbo, C.; Molinaro, R.; Parodi, A.; Toledano Furman, N. E.; Salvatore, F.; Tasciotti, E. The Impact of Nanoparticle Protein Corona on Cytotoxicity, Immunotoxicity and Target Drug Delivery. *Nanomedicine* **2016**, *11*, 81−100.
(73) Docter, D.; Westmeier, D.; Markiewicz, M.; Stolte, S.; Knauer, S. K.; Stauber, R. H. The Nanoparticle Biomolecule Corona: Lessons Learned - Challenge Accepted? *Chem. Soc. Rev.* **2015**, *44*, 6094−6121.
(74) Huhn, D.; et al. Polymer-Coated Nanoparticles Interacting with Proteins and Cells: Focusing on the Sign of the Net Charge. *ACS Nano* **2013**, *7*, 3253−3263.
(75) Garcia, K. P.; Zarschler, K.; Barbaro, L.; Barreto, J. A.; O'Malley, W.; Spiccia, L.; Stephan, H.; Graham, B. Zwitterionic-Coated "Stealth" Nanoparticles for Biomedical Applications: Recent Advances in Countering Biomolecular Corona Formation and Uptake by the Mononuclear Phagocyte System. *Small* **2014**, *10*, 2516−2529.

DOI: 10.1021/acs.jpclett.6b00570
J. Phys. Chem. Lett. 2016, 7, 2139−2150

(76) Algar, W. R.; Medintz, I. Concentric Energy Transfer with Quantum Dots for Multiplexed Biosensing. *Nano Rev.* **2013**, *4*, 22428.
(77) Arnaud, C. H. Analytical Methods Provide Insight into Hazards of Nanomaterials. *Chem. Eng. News* **2010**, *88*, 2780−2799.
(78) Oh, E.; Liu, R.; Nel, A.; Gemilll, K. B.; Bilal, M.; Cohen, Y.; Medintz, I. L. Meta-Analysis of Cellular Toxicity for Cadmium-Containing Quantum Dots. *Nat. Nanotechnol.* **2016**, *11*, 479.

DOI: 10.1021/acs.jpclett.6b00570
J. Phys. Chem. Lett. 2016, 7, 2139−2150